13th International Conference on
Structural Health Monitoring of Intelligent Infrastructure
DOI: 10.3217/978-3-99161-057-1-179

2D sonar techniques for monitoring the canal bed morphology of entrances to navigation locks

Mohsen Bastani[1, ORCID : 0009-0006-9977-7419], Rolands Kromanis [2, ORCID: 0000-0003-3477-1666]
[1]High-Tech Business and Entrepreneurship Department, Industrial Engineering and Business Information Systems, Faculty of Behavioural, Management and Social Sciences, University of Twente, Drienerlolaan 5, 7522 NB Enschede, the Netherlands
[2]The Department of Civil Engineering and Management, Faculty of Engineering Technologies, University of Twente, Drienerlolaan 5, 7522 NB Enschede, the Netherlands
emails: m.bastani@utwente.nl, r.kromanis@utwente.nl

ABSTRACT: Navigation locks are essential components of inland waterways. They enabling vessels to traverse sections with differing water levels. These structures are increasingly vulnerable to damages caused by (1) scour i.e., erosion of sediment due to natural water flow and ship-induced currents, and (2) sediment or debris obstructing lock gates. Scour-induced damage threatens the structural integrity of locks, leading to costly maintenance, prolonged closures, and economic and environmental consequences. Traditional monitoring methods, including visual inspections and fixed instrumentation, are often hampered by water turbidity, high costs, and susceptibility to debris damage. Sonar technologies provide a non-invasive, cost-effective alternative for detailed underwater imaging, even in challenging environments. This paper explores the application of 2D sonar imaging for monitoring navigation lock approaches, with a focus on bed morphology and scour progression. Using the Prinses Beatrix Lock in the Netherlands as a case study, the paper demonstrates the effectiveness of 2D sonar systems in (i) detecting morphological changes such as scour and sediment transport from bed protection layers and (ii) estimating ship drafts. The findings underscore the importance of integrating sonar-based structural health monitoring systems to extend the lifespan of navigation locks, enhance safety, and optimize maintenance strategies for aging waterway infrastructure.

KEY WORDS: sonar technologies; navigation locks; morphological changes; ship draft.

1 INTRODUCTION

Inland waterway transport is significantly more efficient than land-based (i.e., road and rail) transport, as waterways allow for the movement of large cargo volumes with low energy consumption and reduced environmental impact [1]. Navigation locks play a critical role in facilitating inland waterway transport, enabling vessels to traverse sections of canals or rivers with varying water levels. These structures are subjected to various environmental and operational stressors, which can lead to structural deterioration over time. One of the primary concerns in the maintenance of navigation locks is scouring, which is the removal of sediment caused by hydrodynamic forces [2]. Scouring can lead to morphological changes in the bed protection layer, potentially compromising the stability of the lock foundation. The interaction between ship-induced currents and the lock bed remains a significant challenge, particularly for older lock chambers that were not originally designed for large and high-powered vessels [3,4]. The issue is exacerbated by increasing global shipping activities, where vessel sizes and engine power have also grown, leading to intensified hydrodynamic forces in lock approaches [5]. The propeller wash from these vessels accelerates bed degradation, increasing maintenance demands and potential structural risks. The existing bed protection layers, designed decades ago, may not effectively withstand these forces induced by modern vessels.

Traditional monitoring techniques for scouring in navigation locks rely heavily on periodic visual inspections, divers, or stationary sensors. These methods are often costly, labour-intensive, and ineffective in real-time damage detection, particularly in turbid waters where visibility is poor [6]. Some advanced techniques, such as 3D sonar imaging, provide high-resolution data but are prohibitively expensive for widespread implementation. The lack of an affordable and continuous monitoring system leaves lock operators and maintenance teams with limited options for proactive maintenance strategies [7]. The necessity for continuous monitoring of scouring in locks has been well established in existing literature [8], particularly in cases where the structural integrity of the lock foundation is at risk due to progressive erosion.

The issue of sediment transportation in lock complexes, originally designed for smaller vessels, becomes more pronounced with the use of large modern cargo ships. These vessels have a deeper draft, which brings their propellers close to the canal bed. As the vessel moves through the lock, the propeller's interaction with the sediment can cause stones or debris to be displaced and rolled toward the lock chamber. This can result in blockages that obstruct the closure of the lock gates. The presence of such obstructions can cause damage to critical components of the lock system, such as the de-icing pipes [5], which are essential for preventing freezing in cold climates. To prevent such incidents, a continuous monitoring system is essential for detecting these "rolling stones" at an early stage. Such monitoring system is also anticipated to provide insights into how the depth of the ship's draft, which can be correlated with sediment displacement.

To address these issues, an affordable and scalable monitoring system employing 2D sonar imaging has been designed to continuously assess the approach to a lock complex. This novel approach offers scour monitoring, detection of *rolling stones* and estimation of ship's draft in navigation locks. The monitoring system incorporates an image processing algorithm to detect bed morphology changes and provides assessment of vessel-induced impacts on the lock bed.

DOI: 10.3217/978-3-99161-057-1-179

By enabling early detection of bed morphology changes, the system allows for timely interventions and mitigation measures to prevent further degradation of the lock complex. This approach aligns with the broader objectives of structural health monitoring of navigation locks, which aims to extend infrastructure longevity while reducing maintenance costs, thereby enhancing maintenance strategies. The findings of this study can be applied to other navigation locks facing similar challenges, offering a scalable solution for sustainable lock maintenance and improving the overall reliability of inland waterway infrastructure.

2 BACKGROUND

This section explains causes of scour, particularly, in lock complexes, scour monitoring techniques and sonar technologies.

2.1 Scouring

Scour can be categorized into three forms: local scour, contraction scour, and general scour. General scour typically happens as a result of alterations in the natural flow of water, causing the river/canal bed to experience both aggregation and degradation. Contraction scour, on the other hand, is a result of an increase in the flow velocity in conjunction with a reduced cross-sectional area of the waterway. The consequence is the removal of sediment from the waterway's bottom and side [9]. Local scour, the third form, takes place due to turbulent vortices generated by the flow of a current impacting the bed or foundation of the waterway, leading to erosion of surrounding sediment [10].

Local scour is a gradual process that evolves through multiple stages. The initial stage is characterized by the occurrence of erosive effects and damage due to extremely high velocity. Subsequently, scour transitions to the development stage, where the rate of erosion slows down compared to the initial stage. Finally, it reaches the equilibrium stage, where the depth of scour remains stable, and any changes in its depth become imperceptible [11]. The depth of the scour hole in the equilibrium stage is compared with the critical depth of the lock slab or foundation. Local scour takes place in two distinct forms: clear-water and live-bed flow conditions. Differentiating between the two can be determined by observing whether sediment is eroded and replenished (live-bed) or eroded without replenishment (clear-water flow) [10]. The latter condition is often investigated in scour studies.

Local scour is generally linked to turbulent vortices [12–15]. Unlike in cases of bridges, where this turbulence arises from a change in the cross-sectional area of the watercourse due to bridge piers, in locks, the turbulence is caused by the change in the bed roughness introduced by the weir or lock floor. Therefore, structures like locks and weirs, constructed on a soft bed in watercourses, tend to induce local scour, especially in the surrounding bed. To counteract this, a bed protection layer is applied to stabilize the adjacent loose bed.

The intensity of the turbulent vortices generated by this change is directly proportional to the velocity of water flow, higher velocities resulting in greater intensity. In the navigation locks, two factors influence the water flow velocity. Firstly, during the emptying of the lock chamber through small openings, the velocity increases. The intensity of this effect depends on the water level difference between the two sides of the lock. The second factor affecting velocity is the passage of large vessels through the navigation locks. The propeller wash from these large vessels significantly increases water flow velocity, expediting morphodynamical changes in the surrounding bed through scouring. Ships, especially during the initial movement or acceleration, exert the most stress on the bed. Figure 1 (top) illustrates a schematic of a scour hole due to the currents from the emptying of the chamber, and Figure 1 (b) depicts a schematic of a scour hole due to the currents from the propeller wash of entering ships.

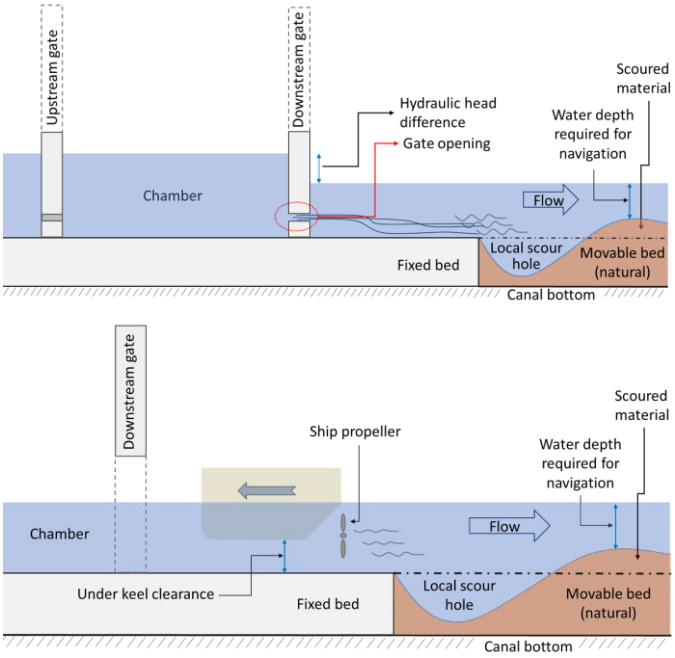

Figure 1. Development of a scour hole downstream of the lock head resulting from (top) currents caused by emptying the chamber, and (bottom) propeller wash of entering ships

When the propellers and thrusters initiate spinning, they set the previously stagnant water in motion. Consequently, they need to overcome the water's initial inertia, leading to the creation of localized vortices and high shear stresses. This shear stress is the cause of bed erosion or scouring. However, once the inertia is surmounted, the stress levels tend to diminish over time [16]. The scour hole generated by the propeller wash can be described as a combination of three polynomial components, including (1) a small scour hole located directly beneath the propeller, (2) a primary scour hole downstream of the initial one, and (3) a deposition mound situated farther downstream of the primary scour hole. This description is based on a setup with non-cohesive sediment [17].

The erosive process of scouring creates a depression in the immediate bed area, and if the slab/foundation's critical depth is surpassed, it can ultimately lead to the undermining and collapse of the foundation. On the other hand, the scoured material can alter the required depth for the navigation of ships. Therefore, in old navigation locks, the scour holes need to be refilled quite often and the sedimentations dredged, otherwise, countermeasures such as a bed protection layer have to be applied. Both scenarios, reduce the efficiency and operability of the lock, causing considerable economic loss [4]. Accordingly, scour holes induced by propeller wash of the

DOI: 10.3217/978-3-99161-057-1-179

ships turned into one of the most prominent concerns for the design and maintenance of the waterways system.

Scour is a complex physical phenomenon involving interactions between flow, structures, and soil. Predictive models for scouring remain unreliable, contributing to the inherent uncertainty in its understanding. Therefore, there is a pressing need for the regular monitoring of scour at critical infrastructures that face a higher risk of scour-induced failure [8]. Continuous monitoring of areas prone to scouring is crucial due to the time-dependent nature of this phenomenon. This helps prevent scour-induced damage from becoming severe and causing critical failures.

2.2 Scour monitoring

The most widespread incidents of scouring in wet infrastructures are related to bridges, which is one of the main causes of bridge collapse [18]. An economically applicable and effective method to combat scouring is to monitor its progress over time and apply countermeasures before poses problems to the structure. The most prevalent monitoring scheme that is commonplace in engineering is visual inspection. In the case of wet infrastructures, visual inspections usually are undertaken by the divers. However, the risk of this inspection method during the flood is high. There is also one important fact about scouring that scour holes might be refilled, accordingly, the strength of the bed is not what it shows in the inspection [7]. Therefore, an effective method could offer continuous monitoring of the depth of scouring. As scour monitoring techniques are relatively well developed for bridge structures, and the origin of failure in locks is the same, the treatment can be generalized to these wet infrastructures as well.

As for bridge scour monitoring, some sensors have been employed that can measure the depth of scour holes such as single-use, pulse or radar, fibre-Bragg grating, driven or buried rod, and sound wave devices [7]. All these sensors are applicable in monitoring the progress of scouring in navigation locks. Among the mentioned methods, the last one; sound wave devices, provides region-wise monitoring, while the rest are spot-wise. In an extensive area such as a lock entrance bed, since the exact spot of scouring is hard to determine, the most promising method is using sound waves or so-called sonar devices [6].

2.3 Sonar techniques for scour monitoring

Sonar is a vital technology used to explore the underwater environment. Sound waves propagate and penetrate more effectively than light through water, especially in conditions of high turbidity. This feature makes it an ideal tool for underwater mapping and detection. Moreover, sound reflection shares similarities with light reflection; surfaces with different textures reflect varying fractions of the incidence of sound. For instance, textured surfaces cause reflection, scattering, and absorption. Surfaces with low reflection have more absorption [19]. The reflecting surface also determines the direction of the reflection. On smooth surfaces, the angle of reflection, measured from the normal to the surface, is equal to the angle of the incident of the wave [20]. However, rough surfaces scatter the waves or reflect them in all directions [19].

Based on the principles of sonar, sonar images can provide information about the location of bed surfaces with (i) strong reflectivity, such as rocks, that (ii) are normal to the sonar transducer (hot/light-coloured pixels). These surfaces may include the uphill side of projections or depressions in the bed. On the other hand, the location of surfaces with low or no reflectivity is also known in the sonar images (cool/dark-coloured pixels). For example, surfaces that are parallel with the sonar transducer, silt or mud-covered areas, areas overshaded by rocks, or the downhill side of depressions and projections. Figure 2 schematically demonstrates reflection intensities against surfaces of the seabed in different directions such as the uphill/downhill facing of projections/depressions.

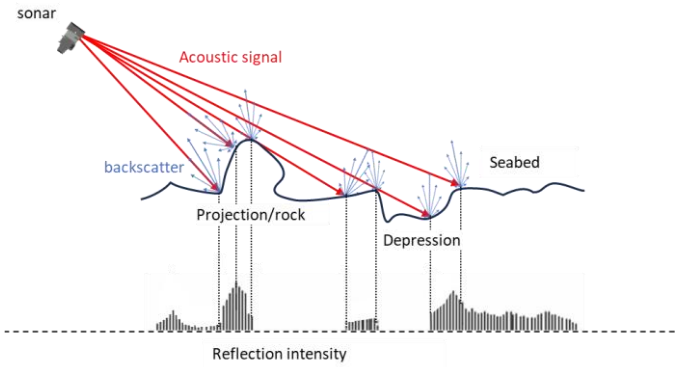

Figure 2. Reflection intensity of acoustic signals

When a rock resting on the waterbed is subjected to a force from high-velocity currents, depending on the weight of the rock, it may undergo displacement from its previous location. In this case, the intensity of signal reflection received by the sonar alters in a specific time interval that is related to a certain location. These alterations occur due to variations in the incident angle of the signals, resulting in modification of the sonar image at that particular location. Additionally, the presence and shape of shadows may undergo changes that indicate a change in the location or orientation of its source. Therefore, by placing a 2D imaging sonar underwater at a suitable altitude and a fixed position facing toward the area of interest on the bed, the changes in the bed features can be captured.

3 THE BEATRIX LOCK COMPLEX

The Princess Beatrix Lock is the largest monumental inland navigation complex in the Netherlands. The lock complex, with three chambers, is located within the Lekkanaal, connecting the Lek River and the Amsterdam-Rhine Canal. This connection is the main and shortest freight corridor and inland waterway between the North of the Netherlands/Amsterdam and Rotterdam/Antwerp. Around 50,000 vessels pass through the lock every year [21]. The Beatrix lock is positioned in the north-south direction, the water flow is northwards. Filling and emptying the lock system is performed via the gates. That means water is brought into or leaves lock chambers through openings in gates, instead of bypassing culverts or stilling chambers. The hydraulic head differences between the two sides of the lock can exceed two meters. Two of the chambers; the twin chambers, with a length of 225 m and a width of 18 m were built in 1938. These chambers can host ships with a maximum draft of 3.5 m. However, the third chamber, built in 2019, is designed to accommodate vessels of CEMT class Vb

DOI: 10.3217/978-3-99161-057-1-179

with a draft of 4 m. The length of the third chamber is 276 m and its width is 25 m. Figure 3 shows an annotated aerial view of the Beatrix lock complex.

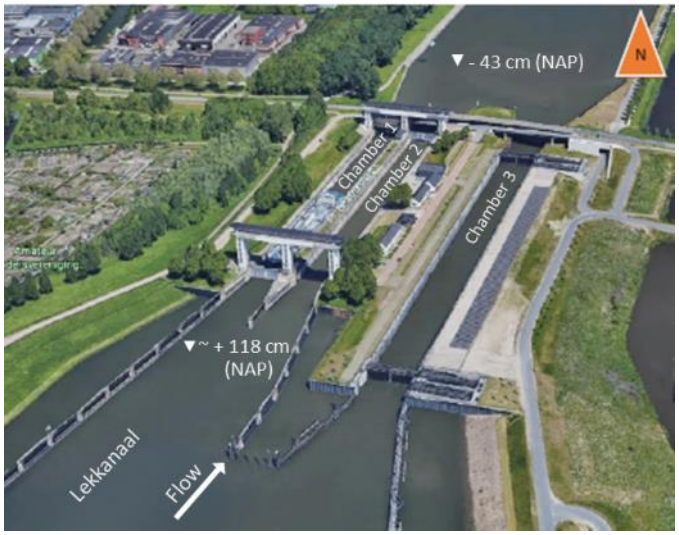

Figure 3. Aerial photo of The Beatrix lock [22]

The filling and emptying system of all three chambers of the Beatrix lock is the opening gate. The gates of the twin chambers have six openings at a height of one meter from the floor of the chamber. The hydraulic head differences between the two sides of the opening are variable and sometimes reach two meters. This difference affects the flow velocity of the opening outlet. In fact, the high-velocity currents from emptying of the chambers (levelling downward) accelerate the progress of scouring at the downstream side of the lock. This is potential damage that occurs due to the operation of the lock by itself, without any ships.

The effect of ship propeller wash on the scouring is intensified by reducing the distance between the ship propeller altitude and the bed. To minimize this effect, a minimum under-keel clearance needs to be considered when the ships pass through the lock. According to the waterways guideline of Rijkswaterstaat, which is the executive agency of the Dutch Ministry of Infrastructure and Water Management, the water depth in navigation canals should be at least a factor of 1.4 times the loaded draft of a passing ship relative to the normal low water level [21]. For example, for ships with a draft of 4 m, the water depth should be at least 5.6 m. This consideration is to minimize the scouring effect of ships' propeller wash on the canal bed. Also, the guideline provides a minimum keel clearance above the chamber floor in locks for different ship categories. For the ships in classes I, II, and III, keel clearance above the chamber floor is 0.6 m, for classes IV to Vb 0.7 m, and for classes VIa and VIb 1.0 m. This consideration needs to be met to minimize the erosion effect of propeller wash related to passing ships.

It is important to know whether the required water depth in the Beatrix lock is in accordance with the guidelines or not. Consequently, the minimum under-keel clearance of the passing ships from the Beatrix lock during the past years of 2019 and 2020 is investigated. To compute the water depth at the moment of passage of ships, the water level and level of the canal bed are needed. By subtracting these two levels, the water depth is determined. In the Rijkswaterstaat database, all the passing ship's details are registered. These details include the date and time of ship entry to the lock, lockage time duration, chamber, direction of passing, and ship category. It is good to mention that ships within the same category have the same loaded draft. However, the status of the ships (loaded/unloaded) is unknown in this dataset.

The level of the canal bed is extracted from a bathymetry map of the lock and surrounding canal. The bathymetry is conducted by Martens en Van Oord in the year 2021. Figure 4 shows a segment of the bathymetry map of the chambers and the approach at the downstream side of the lock. Bed levels at the twin chambers and approach are estimated at -4.62 m and - 4.95 m respectively (these numbers are circled in the figure). Therefore, the water depth of the old chamber during the passage of class VIa ships is on an average between 4.24 m and 4.56 m for the chamber and approach of the lock respectively. However, according to the guidelines, in this case, the water depth should be at least 5.6 m.

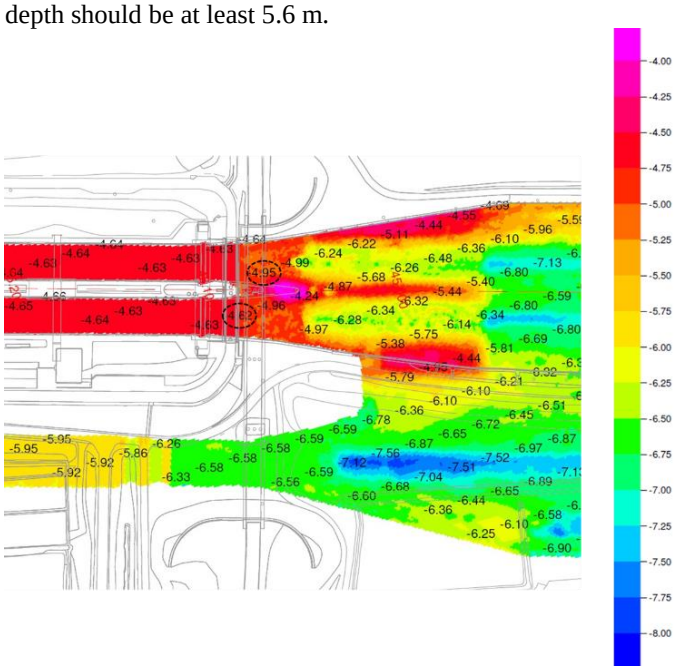

Figure 4. The bathymetry map of the north side of the Beatrix lock (downstream)

To gain insight into the condition of the approach bed of the Beatrix lock, the bathymetry data of the lock is investigated. According to the available drawing from the Beatrix lock in combination with the bathymetry of the canal around the lock structure, there are two changes in the roughness of the watercourse bed along its approach. The first change is related to the junction of the lock head and the bed protection layer of the canal, which is implemented immediately after the lock head. The second change is associated with the junction of the bed protection layer and the natural bed of the canal. Therefore, the junction of these two beds with different roughness is the area where local scour takes place. According to a diver inspection report on the bed protection layer of chambers 1 and 2, the layer is composed of pieces of rock affixed with a cement paste. However, the cement paste does not fully cover the rocks, resulting in a rocky finishing surface.

The point cloud data in Figure 4 from the north side of chamber 1 indicates degradation of the protection layer at its intersection with the natural bed, revealing the progress of the

DOI: 10.3217/978-3-99161-057-1-179

scour hole. While the protection layer on the south side of this chamber shows signs of degradation, the intensity or depth of degradation is not as high as observed on the north side. This difference could be attributed to the lower water depth on the downstream (north side) resulting in more pronounced effects of the ship's propeller wash. The bed protection of the north side of chamber 2 and the south side of chamber 3 have not experienced any significant degradation. However, on the south side of chamber 3, a scour hole has formed at the natural bed of the canal, which could be an initial indication of degradation in the protection layer.

4 SONAR FOR THE LOCK MONITORING

4.1 Selection of sonar device

A variety of sonar devices are available for marine applications such as seafloor mapping, underwater structure inspection, navigation, and commercial fishing [23–26] Given the cost constraint of under €25,000, a 2D sonar was selected for its affordability compared to 3D alternatives.

To identify the most suitable option, 12 commercially available 2D sonar devices were evaluated using a rating system based on criteria including price, frequency, range, power consumption, weight, resolution, casing, field of view, and beam angles. Each device was scored, normalised, and expressed as a percentage. All criteria were equally weighted, as established through requirement analysis. The ISS360 imaging sonar emerged as the optimal choice. Details of the scoring method are provided in Table 1, while the performance results and corresponding ranking are presented in Table 2.

Table 1. The scoring system and the description of the criteria

Score	Field of View (°)*		Score	Frequency (kHz)	
5	360	A wide field of view is preferable, as it leads to reduced number of blind spots and increased coverage area.	3	>/= 900	High frequency is preferable for capturing detailed images of close objects, offering enhanced detail and resolution, while low frequencies are suitable for distant objects.
4	140		2	> 500	
3	130		1	</= 500	
2	120				
1	90				
	Horizontal Beam Angle (°)			**Casing**	
3	</= 0.6	A narrower horizontal beam angle is preferable, as it results in more accurate images at greater ranges.	1	Titanium	Titanium is more durable than aluminum for underwater conditions.
2	</= 1.2		0	Aluminum	
1	> 1.2				
	Vertical Beam Angle (°)			**Weight (kg)**	
5	> 28	A wider angle is preferable for covering a larger area.	3	< 0.5	Light devices are preferable because they require simple and less robust mounts, as opposed to heavy devices, demanding complex and rugged mounting solutions.
4	>/= 26		2	>/= 0.50	
3	>/= 24		1	>/= 1.00	
2	>/= 22		0	>/= 3.00	
1	>/= 20				
0	< 20				
	Operating Range (m)			**Resolution (mm)**	
5	>/= 120	A greater operational range is preferable for achieving more coverage area and higher resolution.	2	< 5 mm	Higher resolution is preferred since it provides more detailed images.
4	> 85		1	</= 10 mm	
3	> 70		0	> 10 mm	
2	> 55				
1	> 40				
0	</= 40				
	Power Consumption (W)			**Price (€)**	
5	< 4	A lower power consumption is preferable for autonomous operating.	4	< 4,000	Lower prices are preferred to ensure that the budget is not exceeded.
4	< 5		3	< 7,000	
3	< 6		2	< 10,000	
2	< 7		1	< 13,000	
1	< 10		0	>/= 13,000	
0	>/= 10				

Table 2. Evaluation results for sonar device selection

	Brand (Model)	Field of View	Horizontal Beam Angle	Vertical Beam Angle	Operating Range	Power Consumption	Frequency	Casing	Weight	Range Resolution	Price	Total Points	score (Out of 100)
1	ImpactSubsea (ISS360)	5	1	2	4	5	2	1	3	1	2	26	**72.2**
2	Echologger (MRS900)	5	1	3	2	4	3	0	2	1	3	24	**66.7**
3	Echologger (RS900)	5	2	5	2	2	3	0	1	1	1	22	**61.1**
4	BlueRobotics (Ping360)	5	1	3	1	3	2	0	2	0	4	21	**58.3**
5	Tritech (Micron Gemini)	1	1	1	1	1	2	0	3	1	1	12	**33.3**
6	Tritech (Gemini 720ik)	2	2	1	5	0	2	0	1	2	0	15	**41.7**
7	Tritech (Gemini 1200iK high-resolution)	2	3	0	1	0	3	0	1	2	0	12	**33.3**
8	Tritech (Gemini 1200iK)	2	2	1	5	0	2	0	1	2	0	15	**41.7**
9	Kongsberg (1171 high resolution)	5	3	5	3	0	3	0	0	1	0	20	**55.6**
10	Kongsberg (M3)	2	2	5	5	0	1	0	0	0	0	15	**41.7**
11	TeledyneMarine (SeaBat F50-R)	4	3	3	5	0	1	0	0	0	0	16	**44.4**
12	Blueview (S M900 Mk2)	3	2	0	5	0	3	0	1	0	0	14	**38.9**

4.2 2D Sonar system

The ISS360 2D imaging sonar from ImapctSubsea is selected as the sonar device for the lock monitoring system. This sonar is a single-beam rotary sonar that scans the area by rotating a transducer via an in-built stepper motor. The transducer emits an acoustic beam with a height of 23° and a width of 2.2° at a central frequency of 700 kHz. It operates within a bandwidth of 600 kHz to 900 kHz and has a range performance ranging from 0.15 m to 90 m. Frequencies below 700 kHz are employed for distances greater than 35 m. Figure 5 shows the geometry of the ISS360 imaging sonar sensor and its fan-shaped acoustic beam.

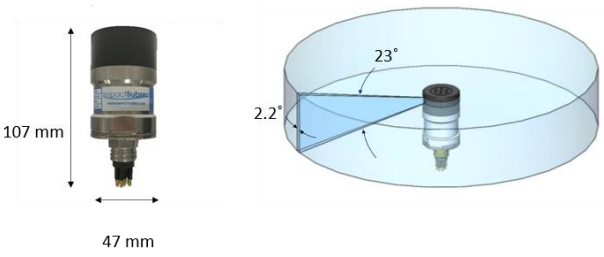

Figure 5. ISS360 imaging sonar sensor and with its principal dimension (left) and beam angles of the sonar (right) [27]

The sonar's power consumption is 150mA at 24V DC during scanning. The sonar device is powered by the Mean Well AC/DC PSU - LRS-75-24 - PSU 1, which outputs 24V/0-3. To enhance its ingress protection (IP) rating, the power supply is enclosed in a (150×110×70 mm) junction box with an IP56 rating. This protective case ensures the power supply can operate in wet environments and raises its IP rating to IP56.

The sonar must be firmly kept in its desired location with minimal vibrations. The sonar mount is specifically designed for this purpose. It restrict the displacement of the sonar to a maximum of 1 mm. This necessitates the mount to be rigid enough to prevent any vibrations or displacement caused by intense ship-induced currents. Another requirement for the sonar mount, associated with the selected sonar device, is to ensure electrical isolation from the housing of the sonar.

Considering the diameter of the sonar (47 mm), two scaffold clamp sizes of 50 mm, coupled with two brackets, are employed as the sonar mount. In one clamp, the sonar is fixed,

DOI: 10.3217/978-3-99161-057-1-179

while in the other clamp, the mount pipe is fixed. The mount pipe can then be affixed to a wall using another clamp and bracket. This coupled clamp system allows the sonar to be positioned and fixed in all orientations. Figure 6 (left) presents the clamp system with sonar and the pipe. To meet the isolation requirement of the mount, a non-conductive spacer (Figure 6 (right)), made of Polylactic Acid, was designed. It is installed between the sonar and the clamp.

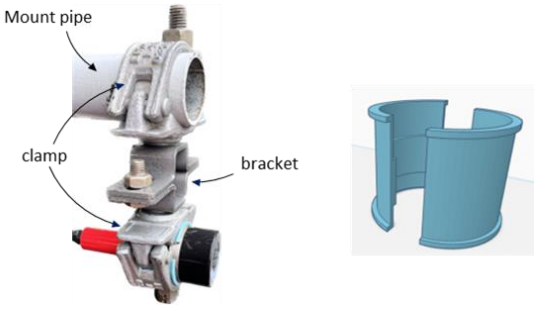

Figure 6. A coupled clamp system with sonar and the mount pipe (left) and a 3D sketch of the spacer (right)

The thickness of the spacer was considered to be 1.5 mm so that, when placed around the sonar, the total diameter of the sonar and the spacer is 50 mm, fitting the size of the clamp. To minimize the risk of the sonar slipping off the mount under high-pressure currents caused by ship propellers, the spacer was designed to provide a firm grip between the sonar and the clamp. The grip between the sonar and the clamp is facilitated by a projection in the spacer that fits into a recess in the sonar housing. Additionally, two teeth were added to the outer side of the spacer to ensure the grip between the spacer and the clamp. Figure 7 shows the detailed design of the spacer. To dampen vibrations between the sonar and the spacer, anti-vibration damper strips were affixed to the spacer. Shows the printed spacer placed between the sonar and the clamp. To prevent self-loosening of the clamp nut and ensure that the sonar remains securely in its place, a spring washer with a double nut configuration is being considered for the clamp

Figure 7. Detailed parts of the spacer

4.3 Sonar location

The north side of chamber 1 is found to be the critical area of concern in the approach bed of the Beatrix lock. The sonar is installed to cover this area. Long-term monitoring of this area may reveal changes in the scour hole in the bed protection layer. The weakness of the protection layer in that region makes it susceptible to further growth, i.e., erosion. The concrete floor of the lock chamber also needs to be included in the sonar's field of view. Such configuration is expected to verify the capability of the monitoring system to capture the deposits on the threshold. If rolling stones/deposits on the concrete floor can be captured, it implies that they can also be captured on the gate threshold. Situating the sonar system between these critical areas ensures comprehensive coverage while considering the trade-off between range limitations and image resolution. Figure 8 provides a top-down view of the point cloud from the north side of chamber 1 superimposed on the drawing of this region. Both the concrete floor of the chamber and the scour hole are illustrated. The location of the sonar is on the east side of the chamber in between the critical areas.

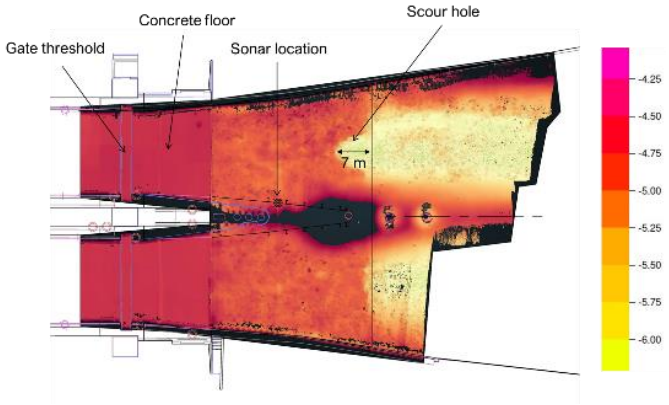

Figure 8. The top-down view of the point cloud of the north side of chamber 1 superimposed on the drawing indicating the sonar location.

The system must not disrupt the operation of the lock. This requirement prohibits any projection of the sonar installation into the track of passing ships. Consequently, the sonar is installed behind the fendering wood of the canal wall. Another requirement is to restrict the sonar displacement to a maximum of 1 millimetre. For this purpose, a galvanized steel pipe 6 m long with a diameter of 50 mm is used for the sonar mount. The mount pipe is clamped at two points to the fendering timbers with a distance of 1 m to provide the required rigidity for restricting vibrations caused by the turbulence of the ship's propeller. Figure 9 (a) depicts a schematic of the sonar installation, providing information about dimensions, while Figure 9 (b) shows an above-water view of the sonar location. Additionally, Figure 9 (c) offers a cross-sectional view of the canal, demonstrating that the outward projection of the sonar does not obstruct the ship's path.

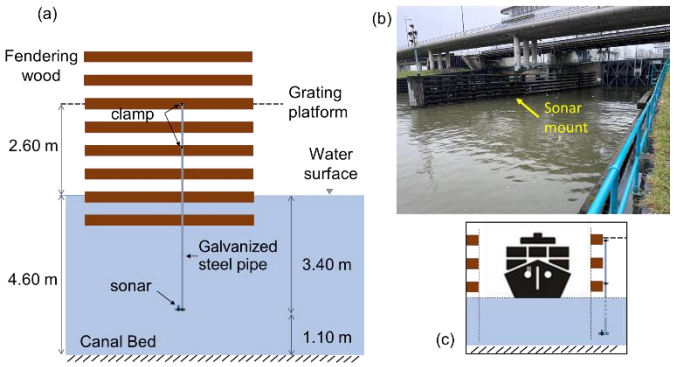

Figure 9. A schematic of sonar installation with some principal dimensions (a), the view of sonar location (b), and projection of sonar toward the ship track (c).

DOI: 10.3217/978-3-99161-057-1-179

5 MONITORING RESULTS

5.1 Changes in the canal bed

The image rendered by the sonar contains two distinct parts; the bed protection layer, where the change in its feature is being sought, and the concrete floor, where the presence of sediment or rolling stone is sought. This section focuses on the bed protection part of the image to evaluate the ability to capture change in bed.

To verify the bed scanning subsystem, over a period of 7 days, the sonar continuously scanned the bed area of interest. Sequential images were acquired by capturing a screenshot from the software window every minute. These images were subsequently compared to evaluate the subsystem's effectiveness in capturing changes in the bed. Effective functionality necessitates, firstly, the absence of any changes in the sequential images as long as no source of excitation, such as the passage of ships or emptying the chamber, occurs. Secondly, changes are expected to occur in the images following a severe excitation.

It is important to note that the emphasis is on changes resulting from the removal of spots with high-intensity reflection, rather than changes due to the appearance of new spots. The removal of spots that have endured for an extended period, signifies their resilience against relocation by heavy ships. The longer a pattern of spots remains in place, the more assuredly it is considered fixed parts of the protection layer. In the event of such changes, it signifies that the initially heavy and securely fixed spot has been relocated due to severe excitation, interpreted as degradation of the protection layer, allowing for the identification of problematic passages. Conversely, the emergence of a new spot suggests a stone coming from elsewhere (probably as a result of removal from somewhere else).

To facilitate image comparison, each sequential image is divided into small ROIs, and each ROI is then compared with the corresponding ROI in the subsequent images. Focusing on only a ROI of this image, for instance, an 8.5 m ×10.5 m area near the scour hole (see Figure 10), numerous green/reddish spots can be seen with specific locations and sizes.

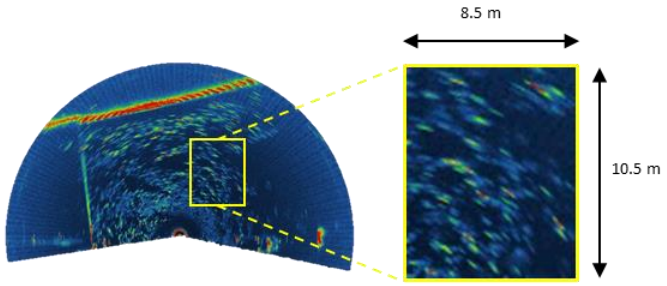

Figure 10. A magnified ROI (yellow box) of the sonar image near the scour hole.

These green spots represent the rock pieces of the bed protection layer. They constitute the distinctive features of the layer, forming a specific pattern depicted in Figure 11 with connected white circles of varying sizes and locations. Upon comparing this pattern in sequential images spanning a 2-day period, no changes are observed. This ongoing steadiness serves as evidence that the level of noise does not compromise image details, thereby satisfying the requirement of a signal-to-noise ratio greater than 1.45. Furthermore, the consistent presence of these green spots, despite various excitations such as ship passages and chamber emptying during this period, indicates that they are fixed components of the protection layer.

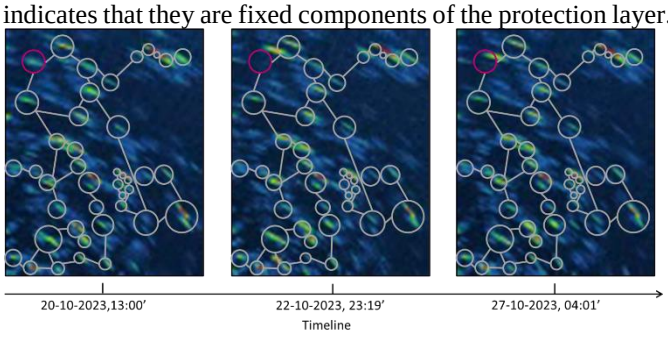

Figure 11. A region of interest in the at three different times, illustrating changes in the fixed pattern of the bed protection.

However, after a ship passage following this period, one of the green spots within this pattern changed its location. Subsequently, the pattern remained unchanged for 5 days. Interestingly, another ship passage after this period led to the same green spot undergoing a change once again. This suggests the presence of a loose stone in the bed protection, potentially indicating degradation of the protection layer. Figure 11 illustrates the initial location of this green spot circled in pink at the measurement's outset and its two new locations after the severe excitations. This serves as compelling evidence of the bed scanning subsystem's functionality, successfully capturing changes in the bed protection layer induced by specific excitations.

It is also possible to identify weak parts of the bed protection layer. For instance, upon an examination of the collected sonar images, specific locations in the bed protection layer exhibited a consistent pattern of spots for 6 days. However, numerous changes in the arrangement of spots, deviating from the fixed pattern, occurred after each passage. This observation indicates the presence of loose stones that are not securely fixed in their location or the void left by a detached stone, subsequently filled with sand. Both scenarios signify a weak section in the bed protection layer.

All constraints of this requirement have been satisfied, specifically, that the system captures changes occurring in at least 3 min within a minimum area of at least 0.5 m². The scanning time for the area of interest at the highest resolution of the sonar device is 1 minute, ensuring the system can capture changes within a 3-minute timeframe. Upon examining the detected change on 27-10-2023, at 04:02', it was found that the change occurred within one minute. In the preceding image, the location of the green spot differed. This change is attributed to a shift in the location of a stone in the bed protection layer, measuring 0.5 m². Figure 12 illustrates the stone in two different locations in two sequential images with a 1-minute interval.

DOI: 10.3217/978-3-99161-057-1-179

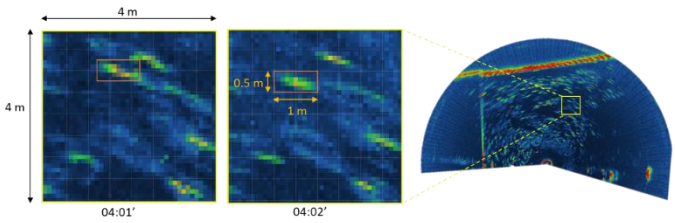

Figure 12. Detected change in the bed protection layer within an area of 0.5m²

5.2 *"Rolling stones" on concrete floor*

This section concentrates on the concrete floor part of the sonar image, aiming to evaluate the subsystem's capability in capturing rolling stones. Upon examining sequential images in this part, a green spot is consistently evident in all images, situated in the north-western part of the concrete floor. This reflection indicates the presence of a projection at that location, as a significant amount of signal is reflected compared to its surroundings, where such reflection is not expected. To confirm this assumption, an underwater drone was sent to that location to capture a video from the concrete floor. The video revealed a substantial piece of rock resting on the concrete floor. Figure 13 (left) presents the identified green spot circled in yellow, and Figure 13 (right) shows a drone-captured image revealing the presence of a substantial rock.

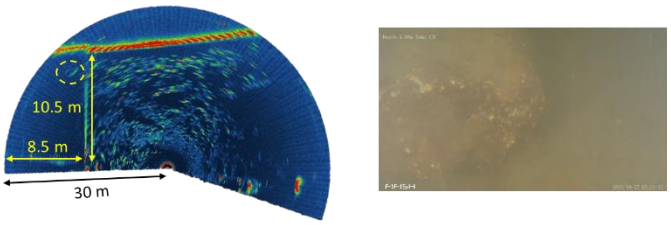

Figure 13. A green spot (circled in yellow) on the concrete floor (left) is a rolling stone, which is captured in an image taken by an underwater drawn (right).

Additionally, certain images display sporadic green spots on the concrete floor, appearing in one image and disappearing in the next. This fleeting presence suggests they are likely fish or other lightweight objects in that area. Contrarily, in many instances, these green spots endure for more than an hour, remaining unchanged in shape and location across many images. This extended presence indicates a heavier object, like stones, in those locations. Figure 14 depicts three incidences of stones observed on the concrete floor. Reviewing images collected over three days of scanning revealed the presence of stones on the concrete floor in multiple instances.

It is noteworthy that the system can capture hills/projections from a distance of 30m. However, the height of the projection cannot be measured due to the lack of access to the stones on the concrete floor captured by the sonar.

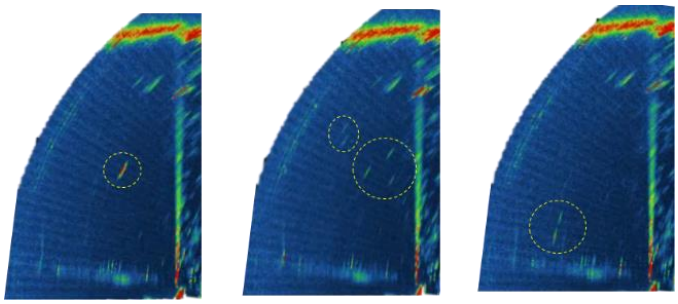

Figure 14. Incidents of persistent green spots (circled in dashed yellow line) suggesting the presence of rolling stones on the concrete floor

5.3 *Ship's draft*

the draft measuring subsystem shares the same components as the bed scanning subsystem. To evaluate the draft measuring subsystem's capability in measuring the actual draft of ships, the sonar was positioned in the same location with a slight modification in its orientation. Due to the inherent limitations of 2D imaging sonar in capturing vertical faces underwater, the sonar mount was tilted 90°, as illustrated in Figure 14 (right), allowing it to render vertical surfaces underwater. In this horizontal orientation, the sonar captures a cross-sectional view of the canal, including the canal bed, wall, and water surface. Figure 14 (left) illustrates the sonar image, overlaid onto the background image, presenting a cross-sectional view of the canal outlined by the red lines. The water surface in the background image is partially cut to reveal a point cloud view of the underwater canal from the same angle. This view allows the observation of the canal wall and bottom.

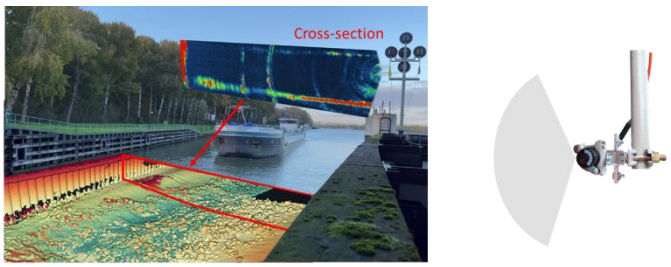

Figure 67 An illustration of a phot combined with 3D point cloud data and the sonar image of the cross-sectional of the canal (left), and the sonar tilted 90° (horizontally mounted) for measuring the ship's draft (right)

When a ship passes the sonar, its hull blocks the sounds, causing a strong reflection due to its surface being perpendicular to the sonar. Consequently, its draft is expected to be captured in the sonar image. Figure 15 (left) presents the sonar image illustrating a cross-sectional view of the canal while a ship is passing the sonar. In this figure, the ship's draft, depicted in red, signifies the extent to which it extends toward the canal bed, providing the dimension of the under-keel clearance. Considering the sonar's depth of 3.5 m, if the ship hull's bottom is not rendered in the image, it implies a draft greater than 3.5 m. Figure 15 (right) displays two passages of large ships with drafts of approximately 3.5 m and 3.6 m. The bottom image, suggesting a larger ship with more draft, blocks the opposite wall completely compared to the top image, despite their equal distance from the sonar.

DOI: 10.3217/978-3-99161-057-1-179

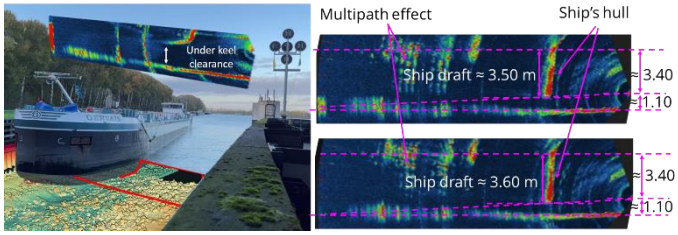

Figure 15. Sonar images rendering the cross-sectional view of the canal during a ship's passage (left) introducing the ship's hull in the sonar image, and estimated draft of two large ships at the same distance from the sonar (right).

Analysing historical traffic data before system design revealed a significant number of large ships passing through the old chambers with drafts of 3.5 m and 4 m. However, this data, obtained from Rijkswaterstaat, did not specify whether the ships were loaded or empty. The difference between loaded and unloaded ships can be up to 2 m. Examining the collected data from measuring ship drafts over 50 hrs uncovered 22 passages of ships with drafts exceeding 3 m, indicating a notable frequency of loaded ships in groups IV and V. Therefore, it is important to note that not all ships with large drafts were necessarily empty.

6 CONCLUSIONS

This project aims to investigate underwater dynamics and ship interactions with the canal bed by visualising changes in the bed protection layer near the lock structure. Reports indicate that this layer consists of large stones fixed with cement, some of which may detach due to excessive water pressure or excitation. Detached stones can obstruct the lock gate, risking damage. Monitoring their movement and understanding the causes i.e., chamber emptying and ship propeller wash, is crucial. The system is designed to detect changes in the bed protection layer, track rolling stones, and measure passing ship's drafts to prevent structural degradation and operational hazards.

The study draws the following conclusions:

- The sonar-based system successfully detects changes in the bed protection layer by capturing consistent images over time. A low noise-to-signal ratio ensures reliable detection, while variations in high-intensity reflections indicate potential degradation caused by ship passages.
- The system can identify and track stones on the concrete floor of the lock chamber. The size of the stones can be estimated using benchmarks, and their movement can be monitored to assess potential risks to lock infrastructure.
- Some ship passages generate significant turbulence, leading to the displacement of stones from the bed protection layer. By correlating these events with sonar images, the system provides evidence that specific passages contribute to degradation.
- Tracking the origin of rolling stones is difficult due to the limited field of view of the sonar. However, adjusting sonar placement and analysing traffic data can help determine whether stones move due to ship passages or chamber emptying.
- By measuring ship drafts and turbulence profiles, the system reveals how propeller wash affects the bed protection layer. High air bubble concentrations in sonar images indicate strong disturbances, which may accelerate degradation of the canal bed.

Future studies should collect a comprehensive dataset using the monitoring system, with at least six months of continuous data to identify change patterns. The current limited dataset provided evidence of bed protection degradation but lacked a complete understanding of the underlying causes. Expanding the investigation to other chambers of the Beatrix lock will reveal trends in scouring and improve detection of loose stones. Implementing automated detection and event correlation will help categorise ship passages, clarifying their role in bed protection degradation.

ACKNOWLEDGMENTS

This research was supported by Heijmans in collaboration with the University of Twente. The authors are pleased to express their gratitude to Dr. ir. Jasper Caerteling for his valuable supervision and to Heijmans Company for their financial and technical support, including facilitating the sonar testing at the Beatrix Lock.

REFERENCES

[1] European Commission. Inland waterways 2025. https://transport.ec.europa.eu/transport-modes/inland-waterways_en.

[2] U.S. Army Corps of Engineers. Engineering and Design: Strength Design for Reinforced Concrete Hydraulic Structures. Engineer Manual* 1110-2-2104. 2023.

[3] Lauth T, Gordon D, Rector M, Moeller W. Scour and subsequent repair at lock & dam 25. 2015.

[4] Mujal-Colilles A, Gironella X, Sanchez-Arcilla A, Puig Polo C, Garcia-Leon M. Erosion caused by propeller jets in a low energy harbour basin. J Hydraul Res 2017;55:121–8. https://doi.org/10.1080/00221686.2016.1252801.

[5] Bastani M. Designing monitoring system for condition assessment of locks. University of Twente, 2024.

[6] Negi P, Kromanis R, Dorée AG, Wijnberg KM. Structural health monitoring of inland navigation structures and ports: a review on developments and challenges. Struct Heal Monit 2023. https://doi.org/10.1177/14759217231170742.

[7] Prendergast LJ, Gavin K. A review of bridge scour monitoring techniques. J Rock Mech Geotech Eng 2014;6:138–49. https://doi.org/10.1016/j.jrmge.2014.01.007.

[8] Yousefpour N, Downie S, Walker S, Perkins N, Dikanski H. Machine Learning Solutions for Bridge Scour Forecast Based on Monitoring Data. Transp Res Rec J Transp Res Board 2021;2675:745–63. https://doi.org/10.1177/03611981211012693.

[9] Liu W, Zhou W, Li H. Bridge scour estimation using unconstrained distributed fiber optic sensors. J Civ Struct Heal Monit 2022;12:775–84. https://doi.org/10.1007/s13349-021-00510-y.

[10] Rogers A, Manes C, Tsuzaki T. Measuring the geometry of a developing scour hole in clear-water conditions using underwater sonar scanning. Int J Sediment Res 2020;35:105–14. https://doi.org/10.1016/j.ijsrc.2019.07.005.

[11] Koken M, Constantinescu G. An investigation of the flow and scour mechanisms around isolated spur dikes in a shallow open channel: 2. Conditions corresponding to the final stages of the erosion and deposition process. Water Resour Res 2008;44:1–16. https://doi.org/10.1029/2007WR006491.

[12] Sui J, Fang D, Karney BW. An experimental study into local scour in a channel caused by a 90° bend. Can J Civ Eng 2006;33:902–11. https://doi.org/10.1139/l06-037.

[13] Park SW, Hwang JH, Ahn J. Physical Modeling of Spatial and Temporal Development of Local Scour at the Downstream of Bed Protection for Low Froude Number. Water 2019;11:1041. https://doi.org/10.3390/w11051041.

[14] Elnikhely EA, Fathy I. Prediction of scour downstream of triangular labyrinth weirs. Alexandria Eng J 2020;59:1037–47. https://doi.org/10.1016/j.aej.2020.03.025.

DOI: 10.3217/978-3-99161-057-1-179

[15] Chang C-K, Lu J-Y, Lu S-Y, Wang Z-X, Shih D-S. Experimental and Numerical Investigations of Turbulent Open Channel Flow over a Rough Scour Hole Downstream of a Groundsill. Water 2020;12:1488. https://doi.org/10.3390/w12051488.
[16] Crowley R, Bloomquist D, Sande S van de, Lescinski J. Characterization of Bed Stresses near Quay Walls Due to Ship Thruster and Propeller Wash. Geo-Congress 2020, Reston, VA: American Society of Civil Engineers; 2020, p. 788–97. https://doi.org/10.1061/9780784482810.082.
[17] Hong J-H, Chiew Y-M, Cheng N-S. Scour Caused by a Propeller Jet. J Hydraul Eng 2013;139:1003–12. https://doi.org/10.1061/(ASCE)HY.1943-7900.0000746.
[18] Lin C, Han J, Bennett C, Parsons RL. Case History Analysis of Bridge Failures due to Scour. Clim. Eff. Pavement Geotech. Infrastruct., Reston, VA: American Society of Civil Engineers; 2014, p. 204–16. https://doi.org/10.1061/9780784413326.021.
[19] Photinos P. The Physics of Sound Waves (Second Edition). IOP Publishing; 2021. https://doi.org/10.1088/978-0-7503-3539-3.
[20] Christ RD, Wernli RL. Sonar. ROV Man., Elsevier; 2014, p. 387–424. https://doi.org/10.1016/B978-0-08-098288-5.00015-4.
[21] Rijkswaterstaat. Richtlijnen Vaarwegen 2020 2020.
[22] Google Maps. The Princess Beatrix Lock arial view 2025.
[23] Stepnowski A, Bikonis K, Moszynski M. 3 D seabed reconstruction from 2 D side-scan sonar images. Forum Acusticum Budapest 2005 4th Eur Congr Acustics 2005:2–6.
[24] Park C, Kim Y, Lee H, Choi S, Jung H. Development of a 2 MHz sonar sensor for inspection of bridge substructures. Sensors (Switzerland) 2018;18:1–9. https://doi.org/10.3390/s18041222.
[25] Manoj A, Aravind H, Varma K, Nair NP, Vivek A, Arjun D, et al. Sonar for Commercial Fishing. 2022 Int Conf Wirel Commun Signal Process Networking, WiSPNET 2022 2022:28–32. https://doi.org/10.1109/WiSPNET54241.2022.9767171.
[26] Horner DP, Healey AJ, Kragelund SP. AUV experiments in obstacle avoidance. Proc MTS/IEEE Ocean 2005 2005;2005. https://doi.org/10.1109/OCEANS.2005.1639962.
[27] IMPACT SUBSEA. IMPACT SUBSEA ISS360 Imaging Sonar Installation & Operation Manual 2021.